

CrystEngComm

Accepted Manuscript



This is an *Accepted Manuscript*, which has been through the Royal Society of Chemistry peer review process and has been accepted for publication.

Accepted Manuscripts are published online shortly after acceptance, before technical editing, formatting and proof reading. Using this free service, authors can make their results available to the community, in citable form, before we publish the edited article. We will replace this *Accepted Manuscript* with the edited and formatted *Advance Article* as soon as it is available.

You can find more information about *Accepted Manuscripts* in the [Information for Authors](#).

Please note that technical editing may introduce minor changes to the text and/or graphics, which may alter content. The journal's standard [Terms & Conditions](#) and the [Ethical guidelines](#) still apply. In no event shall the Royal Society of Chemistry be held responsible for any errors or omissions in this *Accepted Manuscript* or any consequences arising from the use of any information it contains.

ARTICLE

Influence of the coligand in the magnetic properties of a series of copper(II)-phenylmalonate complexes

Cite this: DOI: 10.1039/x0xx00000x

Jorge Pasán,^{a,*} Joaquín Sanchiz,^b Óscar Fabelo,^c Laura Cañadillas-Delgado,^d Mariadel Déniz,^a Pau Díaz-Gallifa,^a Carla Martínez-Benito,^a Francesc Lloret,^e Miguel Julve^e and Catalina Ruiz-Pérez^{a,*}

Received 00th January 2012,
Accepted 00th January 2012

DOI: 10.1039/x0xx00000x

www.rsc.org/

This work presents a series of layered systems based on phenylmalonate-containing copper(II) complexes and different co-ligands. Eight compounds [Cu(L)(Phmal)]_n with L = pyrimidine (pym, **1**), pyrazine (pyz, **2**), 3-cyanopyridine (3-CNpy, **3**), 4-cyanopyridine (4-CNpy, **4**), 3-fluoropyridine (3-Fpy, **5**), 3-chloropyridine (3-Clpy, **6**), 3-bromopyridine (3-Brpy, **7**) and 3-iodopyridine (3-Ipy, **8**), have been synthesized and structurally and magnetically characterized. The coligands selected not only modify the coordination environment of the metal ion, blocking or extending the polymerization, but also interacts with the phenyl ring of the phenylmalonate ligand and affects dramatically the crystal packing through weak interactions. The crystallographic analysis reveals that compounds **1-8** present a corrugated square grid of carboxylate bridged copper(II) atoms where the pyridine ligands are alternatively located above and below each layer and, at the same time, inversely to the position of the phenyl group of the Phmal ligand. It is to remark the fact that the pym and pyz ligands in **1** and **2** do not act as bridges between two copper atoms, whereas weak interactions between the cyano groups are also present in the structures of the complexes **3** and **4**. In compounds **5-8** the increase of the Van der Waals radius of the halogen along the series accounts for the increase of the interlayer separation. Variable-temperature magnetic susceptibility measurements show the occurrence of different magnetic behaviours. Weak interactions are expected for the *anti-syn* carboxylate bridge in the out-of-plane configuration, that can be either ferro- or antiferromagnetic. Therefore, in this manuscript we pretend to shed light to the influence of the magneto-structural relationship in these square grid layered Cu(II) complexes.

Introduction

The construction of coordination polymers (CPs) and metal-organic frameworks (MOFs) is a main area of research aiming at the properties and applications this class of materials can exhibit.¹ Magnetism is one of the attributes this materials can exhibit, and in cooperation with other properties, makes these systems multifunctional. The magnetic properties of coordination polymers derive from the cooperative exchange interactions between the paramagnetic metal ions through the bridging ligands.² In particular, carboxylates have been envisaged both as good linkers in the construction of secondary building units of MOFs and as mediators of the magnetic interaction.³ Therefore, the construction of magnetic systems based on carboxylate ligands has been an active field of research for the last decades. The control of the crystal packing of this coordination polymers is not an easy task. Although the

coordination bond is the primary force to build the metal-organic framework, a tool in which certain control can be exerted, weaker interactions often play an essential role in the assembly process.⁴

The ability of flexible dicarboxylate ligands to build up coordination polymers has been checked with the thorough study of the complexation of the malonate ligand (where malonate stands for the dianion of the propanedioic acid, H₂mal). This ligand has a methylene group between the two carboxylates, a minimal change respect to the rigid oxalate, but with a great influence in the flexibility and versatility. The malonate dianion can then, exhibit a great variety of coordination modes, leading to a great ability to form high dimensional frameworks.⁵ In contrast with the predictable crystal structures rationally designed with the oxalate ligand, the work with a more flexible ligand often gives unexpected results, new coordination modes and unpredictable behaviour

which is the starting point for new polymers with new properties. The magnetic properties of these complexes have been thoroughly studied and magneto-structural correlations have been established.⁶

The inclusion of co-ligands not only modify the coordination environment of the metal ion, blocking or extending the polymerization, but also affects dramatically the crystal packing through weak interactions. To exert some degree of control into the packing of the coordination polymers, subtle modifications, able to establish weak interactions with the surroundings, could be introduced in the polycarboxylate ligand. The malonate ligand has a methylene carbon atom susceptible to accept hydrogen substitutions by other groups like phenyl, benzyl... even aliphatic chains (methyl, ethyl...). This is a fruitful strategy already explored by us and others.^{7,8} In the case of the phenylmalonic acid (H₂Phmal), the presence of a phenyl ring on the methylene carbon group could induce different conformations of the malonate bridging modes due to geometrical constraints and would make possible specific attractive interactions between phenyl rings which would contribute to the overall stability of the resulting compound.⁹ Their role in molecular recognition, and more generally in supramolecular chemistry, has now been widely examined.¹⁰

The aim of this study is to analyze the influence that factors such as the withdrawing effect, the rigidity and the possibility of specific attractive interactions between phenyl rings can exert on the structure and magnetic coupling of phenylmalonate-containing copper(II) complexes. In particular, considering sandwiched systems where a coligand of the pyridine type has been introduced, a strategy based on the reported pyrimidine complex of formula [Cu(pym)(Phmal)]_n (**1**) which exhibits a soft magnet behavior with metamagnetism.¹¹ The layered system observed is the result of hydrophobic interactions, similar to those that form micellar systems, and steric constraints, inherent to the presence of the bulky aromatic group. In this study, we report the syntheses, crystal structures and magnetic properties of a series of eight complexes of formulae [Cu(L)(Phmal)]_n with L = pyrazine (pyz, **2**), 3-cyanopyridine (3-CNpy, **3**), 4-cyanopyridine (4-CNpy, **4**), 3-fluoropyridine (3-Fpy, **5**), 3-chloropyridine (3-Clpy, **6**), 3-bromopyridine (3-Brpy, **7**) and 3-iodopyridine (3-Ipy, **8**), together with a brief discussion of the magneto-structural relationships in square grid layered Cu(II) complexes.

Experimental

Materials and methods

Reagents used in the syntheses were purchased from Aldrich and used as received. Elemental analyses (C, H, N) were performed on a EA 1108 CHNS-O microanalytical analyzer.

Synthetic Procedures

Synthesis of [Cu(pyz)(Phmal)]_n (2**).** An aqueous solution (3 cm³) of copper(II)-phenylmalonate (0.5 mmol, 134 mg) prepared as previously described^{9e} was poured into one arm of a

H-shape tube, whereas a 50/50 water/methanol solution (1 cm³) of pyrazine (0.5 mmol, 40 mg) was added in the other one. The H-shape tube was filled with water and stored at room temperature. Blue plate crystals of X-ray quality were grown after two weeks. Yield 70 %. Anal. calc. for C₁₃H₁₀O₄N₂Cu (**2**): C, 48.52; H, 3.13; N, 8.71%; Found: C, 48.48; H, 3.17; N, 8.70%. IR (cm⁻¹): 2364w, 1588m, 1563s, 1409s, 1331s, 1303m, 1180m, 1033m, 797m, 725s, 697s, 628s.

Synthesis of [Cu(3-CNpy)(Phmal)]_n (3**).** This complex was prepared following the same procedure described for **2**, but using 3-cyanopyridine (0.5 mmol, 55 mg) instead of pyrazine. Pale blue single crystals of **3** in the form of extremely thin plates were grown in the H-shape tube after one month. Yield *ca.* 50%. Anal. calc. for C₁₅H₁₀O₄N₂Cu (**3**): C, 52.10; H, 2.91; N, 8.10%; Found: C, 52.06; H, 3.01; N, 8.05%. IR (cm⁻¹): 1588s, 1560s, 1419m, 1328s, 1180m, 1042w, 816m, 788m, 731s, 691s, 634s.

Synthesis of [Cu(4-CNpy)(Phmal)]_n (4**).** Complex **4** was prepared following the same procedure used for **2** but replacing pyrazine by 4-cyanopyridine (0.5 mmol, 55 mg). Pale blue plate single crystals appear after one month. Yield 50 %. Anal. calc. for C₁₅H₁₀O₄N₂Cu (**4**): C, 52.10; H, 2.91; N, 8.10%; Found: C, 52.15; H, 2.85; N, 8.11%. IR (cm⁻¹): 1670s, 1591s, 1563s, 1432m, 1328m, 1187m, 1067w, 1014w, 826m, 785m, 731s, 694m, 637m.

Synthesis of [Cu(3-Fpy)(Phmal)]_n (5**).** An aqueous solution (3 cm³) of copper(II)-phenylmalonate (0.5 mmol, 120 mg) (which prepared as described in Section 1.1) was set in one arm of a water-fulfilled H-shape tube whereas a 50/50 water/methanol solution (1 cm³) of 3-fluoropyridine (0.5 mmol, 49 mg, 0.043 cm³) was added in the other arm. Pale blue sheet-like poor quality single crystals of **5** appear in the H-tube after two weeks. Yield *ca.* 20%. Anal. calc. for C₁₄H₁₀O₄NFCu (**5**): C, 49.64; H, 2.97; N, 4.13%; Found: C, 49.58; H, 3.01; N, 4.15%. IR (cm⁻¹): 2358s, 1596m, 1560s, 1419m, 1328m, 1183m, 1091w, 1025w, 803m, 728s, 695s, 670s, 631s.

Synthesis of [Cu(3-Clpy)(Phmal)]_n (6**).** Complex **6** was prepared following the same procedure than that described for **5** but using 3-chloropyridine instead of 3-fluoropyridine (0.5 mmol, 57 mg, 0.048 cm³). Pale blue plate single crystals appear after two weeks. Yield *ca.* 60 %. Anal. calc. for C₁₄H₁₀O₄NCICu (**6**): C, 47.34; H, 2.84; N, 3.94%; Found: C, 47.35; H, 2.91; N, 3.93%. IR (cm⁻¹): 2358s, 1590s, 1562s, 1417m, 1328m, 1183m, 1077w, 1023w, 808m, 728s, 699s, 631s.

Synthesis of [Cu(3-Brpy)(Phmal)]_n (7**).** Complex **7** was prepared following the same procedure than that described for **5** but using 3-bromopyridine instead of 3-fluoropyridine (0.5 mmol, 79 mg, 0.048 cm³). Blue plate single crystals appear after two weeks. Yield *ca.* 65 %. Anal. calc. for C₁₄H₁₀O₄NBrCu (**7**): C, 42.07; H, 2.52; N, 3.50%; Found: C, 42.05; H, 2.51; N, 3.51%. IR (cm⁻¹): 2358s, 1591m, 1560s, 1416m, 1328m, 1183m, 1089w, 1020w, 804m, 728s, 694s, 669s, 631s.

Synthesis of [Cu(3-Ipy)(Phmal)]_n (8**).** Complex **8** was prepared following the same procedure than that described for **5** but using 3-iodopyridine instead of 3-fluoropyridine (0.5 mmol,

102 mg). Blue plate single crystals appear after two weeks. Yield *ca* 50 %. Anal. calc. for C₁₄H₁₀O₄NiCu (**8**): C, 37.64; H, 2.26; N, 3.14%; Found: C, 37.65; H, 2.29; N, 3.17%. IR (cm⁻¹): 2358s, 1588s, 1560s, 1453m, 1413m, 1328m, 1183m, 1074w, 1020w, 801m, 728s, 691s, 631s.

Physical Techniques

IR spectra (450–4000 cm⁻¹) were recorded on a Shimadzu IRAffinity1 spectrophotometer equipped with a Pike Technologies GladiATR on powder samples. Magnetic susceptibility measurements on polycrystalline samples, obtained from crushed single crystals, were carried out in the temperature range 1.9–290 K with a Quantum Design SQUID magnetometer. Diamagnetic corrections of the constituent atoms were estimated from Pascal's constants.¹² Experimental susceptibilities were also corrected for the temperature-independent paramagnetism [60 × 10⁻⁶ cm³ mol⁻¹ per Cu(II)] and the magnetization of the sample holder.

Crystallographic Data Collection and Structural Determination

X-ray diffraction data collection on single crystals of **2**, **3** and **6** was performed on a Nonius KappaCCD diffractometer using graphite-monochromated Mo-K α radiation with $\lambda = 0.71073$ Å at 293 K. The data collection of **4**, **7** and **8** were carried out on an Agilent Supernova diffractometer with a copper μ -focus source ($\lambda = 1.5418$ Å). The data were indexed, integrated and scaled with the EVALCCD¹³ (**2**, **3** and **6**) and the CrysAlisPro¹⁴ software programs (**4**, **7** and **8**). The structures were solved by direct methods and refined with a full-matrix least-squares technique on F^2 using the SHELXL-97¹⁵ program included in the WINGX¹⁶ software package. All non-hydrogen atoms were refined anisotropically. The hydrogen atoms were set in calculated positions and refined with a riding model. In the compounds **7** and **8**, there is an unusually high residual electron density we attribute to some twinning combined with the presence of heavy atoms, leading to electron density peaks near the Br and I atoms. The final geometrical calculations and graphical manipulations were carried out with PARST97¹⁷ and DIAMOND¹⁸ programs. A summary of the crystallographic data and structure refinement is given in Table 1. Selected bond distances and angles are listed in Table S1 and S2. Crystallographic data have been deposited at the Cambridge Crystallographic Data Centre with CCDC numbers 996269–996274 for compounds **2–4** and **6–8**, respectively.

Results and discussion

Description of the structures

Compounds 1–4. The structure of the complexes [Cu(L)(Phmal)]_n [L = pym (**1**), pyz (**2**), 3-CNpy (**3**) and 4-CNpy (**4**); see Figures 1 and S1] consists of a sheet-like arrangement of (L)copper(II) units bridged by phenylmalonate ligands running parallel to the *ab* (**1**) and *ac* (**2–4**) planes. A corrugated square grid of copper(II) atoms results (Figure 2) where the pyridine ligands are alternatively located above and

below each layer and, at the same time, inversely to the position of the phenyl group of the Phmal ligand. These sheets are stacked parallel along the *c* (**1**) and *b* (**2–4**) axes, but in **2–4** the sheets are rotated 180° through the *c* direction in a twist fashion (Figure 3) exhibiting the *ABABAB* sequence. The layers are well-separated from each other by means of hydrophobic groups (phenyl groups of the Phmal ligand and the aromatic pyridine ligands) being the interlayer copper-copper separation 13.45(4), 12.413(3), 13.705(5) and 14.039(1) Å in **1–4**, respectively. Weak π -type interactions play an important role in these structures as in that of the previously reported copper(II)-phenylmalonate.^{9e} They occur between the phenyl rings and the pyridine ligands. The aromatic rings are disposed in a face-to-face arrangement with the shortest centroid-centroid distance and off-set angle of 3.74(3) Å and 28.1° (**1**), 4.330(1) Å and 42.6° (**2**), 4.217(5) Å and 30.9° (**3**) and 4.259(1) and 20.50(6)° (**4**), respectively. All these values are in agreement with previous reports on pyridyl-pyridyl interactions.¹⁹ Weak interactions between the cyano groups are also present in the structures of the complexes **3** and **4**. The cyano groups of the CNpy ligands from different layers are symmetry-related by an inversion centre and they exhibit a parallel arrangement. The distances between the midpoints of the C–N bonds are 3.5854(5) (**3**) and 3.7235(1) Å (**4**) and the angles C⁽¹⁾–N⁽¹⁾...C⁽²⁾ are 90.513(3)° (**3**) and 74.1(2)° (**4**). These values are in agreement with those reported for cyano-cyano²⁰ and carbonyl-carbonyl²¹ interactions.

Each copper atom exhibits a square pyramidal environment (the τ values²² being 0.02, 0.006, 0.015 and 0.011 for **1–4**, respectively). Four phenylmalonate oxygen atoms [O(1), O(2), O(3), O(4)] from three different Phmal ligands build the basal plane. The copper-oxygen bond distances in **1–4** are in the range from 1.940(2) Å to 1.9844(15) Å (see Table S1). The apical position is occupied by a nitrogen atom from the pyridine ligand. The copper atom is shifted by 0.2049(10) (**1**), 0.1416(2) Å (**2**), 0.1131(5) (**3**) and 0.1039(5) Å (**4**) from the mean basal plane towards the apical position.

The phenylmalonate ligand acts simultaneously as bidentate [through O(2) and O(4) with the angle subtended at the copper atom being 84.0(3)° (**1**), 87.60(14)° (**2**), 88.16(10)° (**3**) and 88.42(7)° (**4**)] and as bis-monodentate [through O(1) and O(3)]. There are two crystallographically different phenylmalonate-carboxylate bridges [O(1)–C(1)–O(2) and O(3)–C(3)–O(4)], and the mean copper-copper separations through these bridges within the layers are 5.121(17), 5.122(3), 5.111(2) and 5.136(1) Å, for **1–4**, respectively. These values are much shorter than the shortest interlayer metal-metal separations which are in the range of 12.413(3) to 14.039(1) Å.

The sandwich structure of the complexes **1–4** is similar to that of the previously reported copper(II)-phenylmalonate complex^{9e} of formula {[Cu(H₂O)₃][Cu(Phmal)₂]}_n and the series of methylmalonate-containing copper(II) complexes [Cu(Memal)L] (L = H₂O, pyrazine, 4,4'-bipyridine).^{7a} The formation of the square grid of carboxylate-bridged copper(II) ions is only reproduced in the latter series, and it is kept when the coligand is changed.

Let us remark the fact that the pym and pyz ligands in **1** and **2** do not act as bridges between two copper atoms. This is an uncommon situation and, indeed, our goal in the use of these ligands is the reproduction of the results obtained in Co(II) and Zn(II) malonate complexes²³ and $[\text{Cu}_2(\text{Memal})_2(\text{pyz})]^{7a}$ (i.e. the formation of a three-dimensional complex). From a search in the Cambridge Structural Database²⁴ (CSD v.5.35 Feb 2014) we have found that this blocking conformation appears in other 6 (pym) and 7 (pyz) copper(II) complexes among the 44 and 307 which present bridging pym and pyz ligands, respectively. Moreover, if this CSD search is extended to the first-row transition metal ions, only 22 from a total of 126 complexes have a terminal pym ligand in their structure and 37 over 570 complexes do the same with the pyz ligand.

Compounds 5-8. The complexes $[\text{Cu}(3\text{-Xpy})(\text{Phmal})]_n$ [$X = \text{F}$ (**5**), Cl (**6**), Br (**7**) and I (**8**)] are isostructural species and their structure is very similar to those of complexes **1-4** (Figure S2-S5). The structure of **5** could not be solved by single crystal X-ray diffraction measurements (due to the poor X-ray quality of the crystals), but powder X-ray diffraction (see Figure S6) confirms that **5** is isostructural with compounds **6-8**.

As occurs in compounds **1-4** the structure of **6-8** (Figure 3) is made up by a sheet-like arrangement of $[\text{CuL}]$ units [$L = 3\text{-Clpy}$ (**6**), 3-Brpy (**7**), 3-Ipy (**8**)] linked through phenylmalonate ligands running parallel to the *ac* plane. The resulting corrugated layer presents the X-pyridine ligands alternatively located above and below each layer, and inversely to the position of the phenyl group of the Phmal ligand. These sheets, which are stacked along the crystallographic *b* axis in the *ABABAB* sequence, have the odd layers rotated by 180° (Figs. 4 and S4-S5). The layers are well separated by means of the hydrophobic groups, the pyridine-like and the Phmal ligands, the value of the shortest copper-copper interlayer separation being 13.534(2), 13.7673(9) and 14.278(2) Å for **6**, **7** and **8**, respectively. The increase of the Van der Waals radius of the halogen along the series accounts for the increase of the interlayer separation. Weak contacts between the halogen atoms from different layers link the sheets to form a three-dimensional supramolecular structure. With an inversion centre between the halogen atoms, the shortest contacts and angles between them are $\text{Cl}\cdots\text{Cl} = 3.968(4)$ Å and $\text{C}-\text{Cl}\cdots\text{Cl} = 88.8(3)^\circ$ for **6**, $\text{Br}\cdots\text{Br} = 4.042(2)$ Å and $\text{C}-\text{Br}\cdots\text{Br} = 87.97(15)^\circ$ for **7**, and $\text{I}\cdots\text{I} = 4.2512(8)$ Å and $\text{C}-\text{I}\cdots\text{I} = 87.59(14)^\circ$ for **8**. These distances are larger than the sum of Van der Waals radii and the angles are shorter than 90°, suggesting there are other dominant intermolecular forces present in the structure.²⁵ Weak π -type interactions are also present in the structure between Phmal and halogen-pyridine ligands, the shortest centroid-centroid distance and off-set angle being 4.262(6) Å and 33.9(2)° for **6**, 4.238(5) Å and 33.3(2)° for **7** and 4.247(5) Å and 32.6(2)° for **8**, respectively. According to Janiak,¹⁹ these values are within the range of pyridine-type interactions.

Each copper atom exhibits an almost perfect square-pyramidal environment, although that of complex **8** presents a somewhat more distorted surrounding than the other two (the τ value²²

being 0.003, 0.011 and 0.016 for **6**, **7** and **8**, respectively). Four oxygen atoms from three different phenylmalonate ligands [O(1), O(2), O(3) and O(4); mean bond distance being 1.966(8) Å] build the basal plane while a nitrogen atom [Cu(1)-N(1) mean bond distance 2.241(6) Å] occupies the apical position (see Table S2). The copper atom is shifted by 0.1179(9) (**6**), 0.1146(6) (**7**) and 0.1145(7) Å (**8**) from the mean basal plane towards the apical position.

The phenylmalonate ligands adopts simultaneously the bidentate [through O(2) and O(4), the angle subtended at the copper atom being 88.1(2) (**6**), 88.13(13) (**7**), and 88.17(15)° (**8**)] and bis-monodentate coordination modes [through O(1) and O(3)]. Two different phenylmalonate-carboxylate bridges are present within each layer. The one with the O(1)-C(1)-O(2) groups is shorter [Cu···Cu separations through this bridge being 5.0152(13), 5.0059(8) and 5.0028(9) Å for **6**, **7** and **8**, respectively] than that with the O(3)-C(3)-O(4) bridge [5.2585(14) (**6**), 5.2691(8) (**7**) and 5.296(1) Å (**8**)]. It deserves to be noted that the larger is the ionic radius of the halogen present in the ligand, the shorter the copper-copper separation through the O(1)-C(1)-O(2) bridge is encountered. The reverse trend is observed within the O(3)-C(3)-O(4) bridge. These differences could be explained by the distortion of the phenylmalonate ligand. The values of the dihedral angle between the phenyl ring and the basal plane of the copper(II) ion are 83.1(2)° (**6**, 3-Clpy), 83.78(12)° (**7**, 3-Brpy) and 84.63(15)° (**8**, 3-Ipy); the greater the deviation, the larger the distortion between the two bridges.

Let us remark that the 3-Xpy ligands have not a very common use in the coordination chemistry of the first-row transition metal ions, although recently they have been used to build supramolecular copper(II) networks which may exhibit reversible uptake of HCl.²⁶ Of the 55 coordination complexes with the 3-Clpy ligand found in a CSD Database²⁴ search (CSD v. 5.35 Feb 2014), 18 of them exhibit the ligand coordinated to copper ions. In the case of the 3-Brpy ligand, there are 23 reported complexes with this ligand coordinated to transition metal ions and 12 with copper ions. Finally, there are 3 copper complexes among the 15 found with the 3-Ipy ligand, one of them being the one-dimensional methylmalonate-containing copper(II) complex $[\text{Cu}(\text{Memal})(3\text{-Ipy})(\text{H}_2\text{O})]^{7c}$.

Magnetic Properties

$[\text{Cu}(\text{L})(\text{Phmal})]_n$ with **L = pym (1), pyz (2), 3-CNpy (3) and 4-CNpy (4)**. The magnetic properties of complex **1** has been analysed in detail in a previous communication,¹¹ however and for comparison purposes, we have summarized here the main features of its magnetic properties. $\chi_{\text{M}}T$ [χ_{M} being the magnetic susceptibility per copper(II) ion] at room temperature is 0.42 cm³ mol⁻¹ K, a value which is as expected for a magnetically isolated spin doublet. Upon cooling, $\chi_{\text{M}}T$ continuously increases to reach a value of 25.9 cm³ mol⁻¹ K at 2.15 K, and further decreases to 17.5 cm³ mol⁻¹ K at 1.8 K. A maximum in the temperature dependence of the susceptibility is observed at 2.15 K below $H \leq 130$ G. A maximum that disappears when external magnetic fields above 130 G are applied. These features

correspond to a metamagnetic-like behaviour which is due to the coexistence of ferro- and antiferromagnetic interactions, the latter one being overcome by an external magnetic field higher than 130 G. The sigmoidal shape of the magnetization (M) versus H plot at 1.8 K at very low magnetic fields confirms this metamagnetic behaviour. The proposed exchange pathways for the ferromagnetic interactions correspond to the carboxylate-bridges that form the square grid of copper(II) ions and the fitting through a high-temperature expansion series²⁷ leads to $J = +5.6(1) \text{ cm}^{-1}$, $g = 2.12(2)$. The small antiferromagnetic interaction should correspond to the coupling of the ferromagnetic layers with a main dipolar character given the lack of hydrogen bonds or π -type interactions between the layers.

The magnetic properties of **2** under the form of $\chi_M T$ vs. T plot [χ_M being the magnetic susceptibility per copper(II) ion] are presented in Figure 5. The value of $\chi_M T$ at room temperature is $0.42 \text{ cm}^3 \text{ mol}^{-1} \text{ K}$, a value which is as expected for a magnetically isolated spin doublet. Upon cooling, $\chi_M T$ smoothly increases to reach a maximum of $0.50 \text{ cm}^3 \text{ mol}^{-1} \text{ K}$ at 19 K, then the $\chi_M T$ product sharply decreases to $0.12 \text{ cm}^3 \text{ mol}^{-1} \text{ K}$ at 2.0 K. A susceptibility maximum is observed at 3.5 K which disappears for magnetic applied fields above 3 T. These features are very similar to those observed in **1**, and the same phenomenon is present here. A metamagnetic-like behaviour occurs in **2** due to the coexistence of ferro- and antiferromagnetic interactions, the latter being overcome for $H > 3 \text{ T}$. The magnetization (M) vs H plot at 2.0 K for **2** confirms this assumption showing a sigmoidal shape with an inflection point at $H_c = 3.6 \text{ T}$ (Figure 6). An estimation of the magnitude of the interaction can be obtained from H_c , being *ca.* 3.2 cm^{-1} , of the same order than the ferromagnetic coupling parameter through the *anti-syn* equatorial-equatorial carboxylate bridge for previously observed for $\{[\text{Cu}(\text{H}_2\text{O})_3][\text{Cu}(\text{Phmal})_2]\}_n$ and for compound **1** [J being $+4.15(2)$ and $+5.6(1) \text{ cm}^{-1}$, respectively],^{9e,11} as well as other related malonate complexes.^{6,7} The linearity of the magnetization at applied fields below the inflexion point is indicative of this antiferromagnetic coupling.

Bearing in mind the previous considerations, the magnetic behaviour of **2** can be viewed as the competition of two interactions of opposite nature which operate within the carboxylate-bridged layers of copper(II) ions. Since there are two different *anti-syn* carboxylate bridges in the structure, one of them must couple the copper(II) ions ferromagnetically and the other one antiferromagnetically. Thus, from a magnetic point of view, the layers of compound **2** consist of a square grid with two magnetic interactions of different nature. As there is no theoretical equation to analyse these data, we can model the system as cross-linked AF and F chains. This situation can be analyzed through the Baker and Rushbrooke numerical expression²⁷ for a ferromagnetically coupled copper(II) chain with an additional mean-field term which takes into account the AF interaction²⁸ (an approximation that must be taken with care since the two coupling parameters are of the same order of magnitude).

$$\chi_{2D} = \frac{\chi_{1D}}{1 - (2zj/Ng^2\beta^2)\chi_{1D}} \quad (1)$$

$$\chi_{1D} = (Ng^2\beta^2/4kT)(A/B)^{2/3} \quad (2)$$

with $A = 1.0 + 5.7979916 y + 16.902653 y^2 + 29.376885 y^3 + 29.832959 y^4 + 14.036918 y^5$ and $B = 1.0 + 2.7979916 y + 7.0086780 y^2 + 8.6538644 y^3 + 4.5743114 y^4$; when the Hamiltonian considered is:

$$\hat{H} = -J \sum_i \hat{S}_i \cdot \hat{S}_{i+1} \quad (3)$$

with $y = J/2kT$. J and j are the intrachain and interchain magnetic coupling parameters, respectively, $z = 2$, is the number of nearest neighbours. The other symbols have their usual meanings. Best least-squares fit parameters for the temperature range 20 to 300 K are $g = 2.072(4)$, $J = +10.4(1) \text{ cm}^{-1}$, $j = -3.19(5) \text{ cm}^{-1}$ and $R = 8 \times 10^{-4}$. The calculated curve match well the experimental data in the temperature range considered as shown in Fig. 5.

The temperature dependence of the $\chi_M T$ products [χ_M being the magnetic susceptibility per copper(II) ion] for the complexes **3** and **4** in the temperature range 1.9-300 K are shown in Figures 5 and 7, respectively. The $\chi_M T$ product at room temperature is $0.41 \text{ cm}^3 \text{ mol}^{-1} \text{ K}$ for **3** and **4**, a value which is as expected for a magnetically isolated spin doublet. This value remains constant for **3** until 150 K and then smoothly increases to reach a maximum value of $0.61 \text{ cm}^3 \text{ mol}^{-1} \text{ K}$ at 5.5 K, and finally it decreases sharply to a value of $0.55 \text{ cm}^3 \text{ mol}^{-1} \text{ K}$ at 2.0 K. This is indicative of the coexistence of ferro- and antiferromagnetic interactions. The magnetization (M) vs H plot for **3** at 2.0 K shows a sigmoidal shape indicating the occurrence of a metamagnetic-like behaviour (Figure 6) with an inflexion point at $H_c = 1.0 \text{ T}$. The sharp increase after H_c to reach the saturation value of 1.10 BM at 4.0 T supports the presence of ferromagnetic interactions between the spin doublets. The value of the critical field H_c accounts for an antiferromagnetic coupling of $-0.70(1) \text{ cm}^{-1}$. The situation for **4** is slightly different, the $\chi_M T$ value at room temperature is kept almost constant up to 50 K and then $\chi_M T$ abruptly increases to reach a value of $1.82 \text{ cm}^3 \text{ mol}^{-1} \text{ K}$ at 2.0 K. This indicates an overall ferromagnetic behaviour. The magnetization curve at 2.0 K for **4** does not exhibit the sigmoidal shape and it reaches the saturation value at 3.5 T (see Fig. 6).

The magnetic behaviour of **3** is very similar to that of **2**, where the competition of two interactions of opposite nature is also present. This situation can be analyzed using the same approach, through the Baker and Rushbrooke numerical expansion series together with a mean-field term (eqs. 1-3).^{27,28} This approach is reliable only in the temperature range from 4 to 300 K. The best least-squares fit parameters in the whole range of temperatures are $g = 2.052(2)$, $J = +6.3(1) \text{ cm}^{-1}$, $j = -0.82(1) \text{ cm}^{-1}$ and $R = 2 \times 10^{-4}$. The calculated curve fit well the experimental data in the range 4-300 K (Figure 5), but at lower temperatures there are some discrepancies since the model have not taken into account the antiferromagnetic interaction between layers. However, the obtained values are in agreement

with the calculated AF coupling estimated from the value of the critical field of $H_c = 1.0$ T [$j = -0.70(1)$ cm⁻¹] as well as with the value of the ferromagnetic coupling of compound **1** and other related copper(II)-malonate complexes.^{6,7,9,11}

The magnetic behaviour of **4** would correspond to that of a ferromagnetically coupled square grid of copper(II) ions through carboxylate-bridges in the *anti-syn* conformation. Consequently, the magnetic data of **4** were analyzed through the expression of the magnetic susceptibility derived from the high-temperature expansion series for an isotropic ferromagnetic square lattice with interacting spin doublets together with a mean-field term.²⁹ The spin Hamiltonian is defined in eq. 3 and the series takes the form:

$$\chi = \left(\frac{N\beta^2 g^2}{3k_B T} S(S+1) \right) \left[1 + \sum_{n \geq 1} a_n \frac{x^n}{2^n} \right] \quad (4)$$

where N , g , β and k_B have their usual meanings, $x = J/k_B T$, J is the intralayer magnetic coupling and a_n are coefficients which run up to $n = 10$. Least-squares fit of the experimental data leads to $J = +1.69(2)$ cm⁻¹, $g = 2.14(2)$, $j = -0.26(1)$ cm⁻¹ ($z = 2$ in this case) and $R = 9 \times 10^{-4}$. The calculated curve matches very well the experimental data in the whole temperature range (Fig. 7). The value of J for **4** is in agreement with the observed in the family of carboxylate(phenylmalonate)-bridged copper(II) complexes [J ranging from $-0.59(1)$ to $+4.44(5)$ cm⁻¹]⁹ and it lays within the range of the previously reported magnetic interactions for the *anti-syn* carboxylate(malonate)-bridged copper(II) complexes.^{6,7,11}

Since there are two crystallographically different carboxylate-pathways bridging the copper atoms within the layer in **4**, it is possible that they would have also different magnetic interactions as in compounds **2** and **3**. The series expansion used in the previous fit considers both exchange pathways to be equivalent; nevertheless the same model used previously with **2** and **3** could be used in order to take into account the two bridges with different magnetic couplings. The experimental data of **4** have been fitted using eqs. 1-3. The best least-squares fit parameters are $g = 2.060(5)$, $J = +6.0(1)$ cm⁻¹, $j = +0.070(4)$ cm⁻¹ and $R = 2 \times 10^{-4}$. In this case, both fits match very well the experimental data in the whole temperature range as can be seen in Fig. 7. However, for the latter fit, the value of j should be taken carefully since it may include some interactions between the layers through π - π stacking and cyano-cyano contacts, as occurs in **1**.

The magnetic interactions between the copper atoms through the equatorial-equatorial *anti-syn* carboxylate bridge observed in **3** and **4** are in agreement with the data reported in the literature for copper(II) complexes with this kind of bridge (see Table 2 and discussion below).^{6,7,9,30}

[Cu(3-Xpy)(Phmal)]_n with X = F (**5**), Cl (**6**), Br (**7**), I (**8**).

The magnetic properties of compound **6** under the form of $\chi_M T$ vs T plot [χ_M being the molar susceptibility per copper(II) ion] are shown in Figure 8. $\chi_M T$ at room temperature is 0.39 cm³ mol⁻¹ K, a value which is as expected for a magnetically

isolated spin doublet. Upon cooling, $\chi_M T$ remains almost constant up to 20 K and then, it smoothly decreases to reach a value of 0.32 cm³ mol⁻¹ K at 1.9 K. The temperature dependence of the $\chi_M T$ product for compounds **5**, **7** and **8** are shown in Fig. 8. At room temperature, the values of $\chi_M T$ are 0.41 , 0.42 and 0.43 cm³ mol⁻¹ K for **5**, **7** and **8**, respectively. These values remain constant upon cooling until 100 K, and then smoothly increase to reach a maximum of 0.50 cm³ mol⁻¹ K at 11 K for **5**, 0.60 cm³ mol⁻¹ K at 6.5 K for **7** and at 0.58 cm³ mol⁻¹ K at 7.0 K for **8**. At lower temperatures, the $\chi_M T$ curves sharply decrease to reach values of 0.23 (**5**), 0.44 (**7**) and 0.38 (**8**) cm³ mol⁻¹ K at 2.0 K. The magnetic behaviour of **6** is indicative of the existence of antiferromagnetic coupling between the copper(II) ions. However, the situation for **5**, **7** and **8** is rather different, where there is a competition between two interactions, ferro- and antiferromagnetic. The magnetization (M) curve for **6** lays under the Brillouin function for a magnetically isolated spin $S = 1/2$ in the entire range of the magnetic field available (0-5 T). However, the M vs. H plot for **5**, **7** and **8** shows the sigmoidal shape characteristic of a metamagnetic-like behaviour (Fig. S7). The saturation of the magnetization is reached at an applied field of 4.5 T.

The distinct magnetic behaviour of **6** compared with all the previously reported compounds with a layered structure of carboxylate bridged copper(II) ions can be explained if the antiferromagnetic exchange coupling is greater than the ferromagnetic one. Then, the magnetic data of this system can then be analyzed by means of Fisher expression³¹ for an antiferromagnetically coupled regular chain of copper(II) ions with a mean-field term (eq. 1) to take into account the second exchange pathway with $z = 2$:

$$\chi_{1D} = \left(\frac{N g^2 \beta^2}{k_B T} \right) \left[\frac{0.25 + 0.074975x + 0.075235x^2}{1 + 0.9931x + 0.172135x^2 + 0.757825x^3} \right] \quad (5)$$

where N , β , g and k_B have their usual meanings, $x = |J|/k_B T$ and J and j are the magnetic coupling parameters. Best least-squares fit of the experimental data leads to $J = -0.91(3)$ cm⁻¹, $j = +0.27(3)$ cm⁻¹, $g = 2.059(1)$ and $R = 8.3 \times 10^{-5}$. The calculated curve matches the experimental data well (Figure 8). Although the difference between the two magnetic coupling parameters obtained in the fitting is not large enough to validate the model used, it is remarkably that they are different in nature. The largest coupling is antiferromagnetic, thus it dominates the magnetic behaviour observed in **6**.

The coupling parameters $J = -0.91(3)$ cm⁻¹ and $j = +0.27(3)$ cm⁻¹ obtained are within the range of those reported for a carboxylate bridge in *anti-syn* conformation which links two equatorial positions of the copper(II) environment.^{6,7,9,30} According to the Kahn's orbital model,³² the counterbalance of the ferro- and antiferromagnetic contributions is so delicate that small variations of structural features can favor the overlap and then make the antiferromagnetic contribution to predominate as occurs in **6**.

The magnetic behaviour of compounds **5**, **7** and **8** are very similar and reminiscent of that of **2** and **3**. Thus, there is a

competition between two interactions of opposite nature which operate through the carboxylate-bridged layers of copper(II) ions. The two crystallographically different carboxylate bridges within the layers must couple the copper(II) ions ferro- and antiferromagnetically. Then, under a magnetic point of view, the layers of **5**, **7** and **8** can be seen as cross-linked AF and F chains. An analysis through the Baker and Rushbrooke numerical expression for a ferromagnetically coupled copper(II) chain with a mean-field term to take into account the interchain interactions (eqns. 1-3)^{27,28} was performed. The best least-squares fit parameters are $g = 1.981(4)$, $2.076(2)$ and $2.055(2)$, $J = +9.0(1)$, $+6.3(1)$ and $+6.8(1) \text{ cm}^{-1}$, $j = -1.083(8)$, $-0.929(2)$ and $-1.089(3) \text{ cm}^{-1}$ and $R = 9 \times 10^{-4}$, 4×10^{-4} and 8×10^{-4} for **5**, **7**, and **8**, respectively. Even thinking that the model fittings match well the experimental data in the whole temperature range as can be seen in Fig. 8, the values of J and j must be taken with caution due to the rough character of the approaches used. The antiferromagnetic coupling constant can be estimated from the critical field [$H_c = 2.4$ (**5**) and 1.2 T (**7** and **8**)] being $j \sim -1.1 \text{ cm}^{-1}$ for **5** and $j \sim -0.6 \text{ cm}^{-1}$ for **7** and **8**. These values are similar to that obtained from the analysis of the antiferromagnetically coupled copper(II) layers in complex **6**.

There is a delicate equilibrium between the ferro- and antiferromagnetic interactions in these four complexes. The magnetic coupling parameters range in the $[2.4 \text{ cm}^{-1}]$ span, and they are in agreement with those reported for exchange pathways through carboxylate in *anti-syn* conformation.^{6,7,9,30} Thus, subtle changes in the structure, such as the distortion environment, axial bond distance, planarity of the basal plane, dihedral angle of the carboxylate bridge, and so on, could make the ferro- (**5**, **7** and **8**) or antiferromagnetic (**6**) contribution to predominate.

Magneto-structural discussion

Let us briefly discuss the main structural features of this series of complexes and their influence in the magnetic behaviour. The complexes of this comparative analysis are displayed in Table 2 (Figure 9). They all share some structural details apart from the Cu(II) square-grid layered conformation, all the equatorial ligands are oxygen atoms from R-malonate ligands, the carboxylate bridges exhibit the *anti-syn* conformation with a certain degree of out-of-plane configuration, and the axial positions are occupied by pyridine-type or water molecule ligands. In Table 2, compound **5** has been omitted because of the lack of structural details.

Considering the results listed in the Table 2, the magnetic exchange couplings through the carboxylate bridges range from -1.089 to $+6.8 \text{ cm}^{-1}$. These values are in agreement with those reported in the literature for *syn-anti* carboxylate bridges linking equatorial positions at the copper(II) environment.^{6,7,9,30} They are also in accordance with the classical magnetic orbital explanation with accidental orthogonality.^{3e,6a,32} However, what is a more difficult task is to evaluate the structural feature responsible for the small changes in the magnetic coupling parameter from one compound to another.

Comments on the Crystal Structure. First of all, let us compare some structural features among the complexes and the reasons for specific changes to appear.

Copper(II) environment. All the complexes exhibit square pyramidal surroundings with very small distortions. A close look to the Cu–O bond distances reveals that they subtly vary among the complexes, the longer equatorial Cu–O bond distances correspond to **8** and, in general, they range from $1.940(3)$ to $2.001(4) \text{ \AA}$.

Carboxylate bridged copper(II) separations. The Cu⋯Cu separations through the carboxylate bridge are slightly different from one compound to another but, more interestingly, also between the two crystallographically independent carboxylate bridges of the same complex. The values for the Cu⋯Cu separation through the carboxylate exchange pathway in these complexes range from $4.842(5)$ to $5.296(1) \text{ \AA}$. The greatest difference between the Cu⋯Cu separations between the two carboxylate pathways in a given complex occurs in **8**, which represents an extreme situation in the sub-series of the halogenpyridine complexes where the short and long carboxylate-bridges decrease and increase in length, respectively, along the series Cl, Br, I. The carboxylate bridges are only equivalent in the reported complexes $[\text{Cu}(\text{Memal})(\text{H}_2\text{O})]_n$ and $[\text{Cu}(\mu\text{-cbdca})(\text{H}_2\text{O})]_n$.

Conformation of the carboxylate bridge. The dihedral angle between the basal plane of the copper atom and the carboxylate bridge is always smaller in the *anti* side (where the copper atom is chelated) (first value of γ in Table 2). This value is shorter in the complexes of methylmalonate and cyclobutanemalonate than in those of phenylmalonate. The average of this angle in the copper(II)-malonate complexes is 24.6° ,[†] while in the case of the oxalate compounds, it is close to 0° . Therefore, this value increases subtly but significantly with the bulkiness of the substituent. The angle between the basal plane of the copper atom in *syn* conformation and the carboxylate bridge ranges from $61.88(18)$ to $82.4(5)^\circ$. The whole situation corresponding to an out-of-plane configuration of the *syn-anti* bridge.

Angle between basal planes of carboxylate bridged copper(II) ions. As a consequence of the out-of-plane configuration of the bridge the basal planes of the copper(II) ions are nearly perpendicular favouring the accidental orthogonality of the magnetic orbitals. This angle ranges from $63.16(2)^\circ$ to $84.44(9)^\circ$. The higher values occur in the methyl- and cyclobutane-malonate complexes.

Interlayer separations. The Cu⋯Cu separations between layers are determinately influenced by the coligand. The interlayer distance grows according to how bulky is the group attached to the pyridine ring as occur in the series [3-Clpy (**6**), 3-Brpy (**7**) and 3-Ipy (**8**)], also the position of the group in the pyridine ring plays an important role [the separation with the 3-CNpy (**3**) is shorter than that with the 4-CNpy (**4**)].

Comments on the Magnetic Behaviour. The assignation of a general trend in the magnetic properties in relation with the structural parameters on this series of compounds is not evident. There are many structural parameters involved (see

Table 2) which can vary simultaneously, some to favour the ferromagnetism and others to increase the antiferromagnetic contribution. It is worth mentioning that we have to be cautious with the values of the coupling constants listed in Table 2 because they come from analyses with different theoretical models.

There are not many structural differences between complexes **1-4**. They are built up from the phenylmalonate ligand with pyrimidine, pyrazine and cyanopyridine as coligands, and they all show moderate ferromagnetic interactions. A weak antiferromagnetic interaction can coexist, in **1** it was assigned to a through-space interlayer interaction and to intralayer exchange pathways in **2** and **3**. The occurrence of this weak contribution is not evident in **4**, but if any it becomes very weak whether ferro- or antiferromagnetic. The reasons for these changes are difficult to found out in the structural parameters listed in the Table 2. We can see how the dihedral γ angle of the chelating carboxylate slightly decreases along the series, pym, pyz, 3-CNpy and 4-CNpy, at the same time the β angle between the two connected copper(II) ions smoothly increases. Probably, **1** is the complex with a more different conformation of the carboxylate bridge (see the γ angles in Table 2), and indeed this is the unique complex which exhibits a large magnetic correlation and magnetic ordering below 2.15 K. The Figure 9 shows the superposition of fragments of the structure of complexes **1-4**. There exists differences, but they are very subtle and involve the location of the phenyl ring of the phenylmalonate ligand and the pyridine ring, being these variations due to supramolecular interactions. Therefore, we can see how the introduction of a specific group which is able to establish supramolecular interactions can modify the structure of the carboxylate exchange pathway and then alter the magnetic properties observed.

The complexes **6**, **7** and **8** are built up from phenylmalonate complexes with halogen-pyridine coligands. The interaction among the copper(II) ions in **6** is mainly antiferromagnetic, whereas in **7** and **8**, ferro- and antiferromagnetic interactions coexist. The structures of these compounds are very similar with no remarkably changes in the conformation of the bridge, and just an enlargement of the carboxylate exchange pathway and the Cu–O bond distances along the series Cl, Br, I. The magnetic behaviour of **6** was analysed in terms of two interactions of approximately the same magnitude and opposite nature (see Magnetic Properties Section). This situation is similar to that observed in **5**, **7** and **8**, with the exception that in these latter compounds the ferromagnetic interaction is strong enough to be observed in the magnetic susceptibility measurements. This suggests that only very subtle changes in the structural configuration are necessary to overcome the ferromagnetism and make the antiferromagnetic contribution to dominate, as occurs in **6**.

Looking at the picture with perspective, including the two related compounds $[\text{Cu}(\text{Memal})(\text{H}_2\text{O})_n]$ and $[\text{Cu}(\mu\text{-cbdca})(\text{H}_2\text{O})_n]$, two-dimensional ferromagnetic systems (with two ferromagnetic carboxylate bridges) exhibit two *anti-syn* carboxylate bridges with very similar Cu···Cu separations. In

the two reported compounds, they are crystallographically equivalent, but in **1**, the two copper separations are alike. In the rest of compounds, there is a bridge with a higher Cu···Cu separation than the other. This seems to be related with the occurrence of an antiferromagnetic interaction. However, theoretical simulations are needed to unambiguously assign the longer bridge to the AF interaction. In general, there are many structural parameters involved which can vary simultaneously along the series of compounds, some to favour the ferromagnetism and others to increase the antiferromagnetic contribution.

Conclusions

In the present paper, we have discussed the syntheses, crystal structures, and magnetic behavior in the temperature range 2–300 K of eight metal-organic 2D polymers, consisting of a sheet-like arrangement of (L)copper(II) units bridged by phenylmalonate ligands, forming as structural motif a corrugated square grid of copper(II) atoms. They all share some structural details apart from the main layered conformation; all the equatorial ligands are oxygen atoms from R-malonate ligands, the carboxylate bridges exhibit the *anti-syn* conformation with a certain degree of out-of-plane configuration, and the axial positions are occupied by pyridine-type or water molecule ligands. From the magnetic point of view the complexes exhibit magnetic couplings through the carboxylate bridges ranging from -3.19 to $+10.4(1)$ cm^{-1} . We can see how the introduction of different groups able to establish supramolecular interactions can modify the structure of the carboxylate exchange pathway and then alter the magnetic properties observed. Except for compound **1**, there is a delicate equilibrium between the ferro- and antiferromagnetic interactions in complexes **2-8**. In order to understand this behaviour, an analysis of magneto-structural relationships has been done, unfortunately appears that there are many structural parameters involved which can vary simultaneously along the series of compounds, some to favour the ferromagnetism and others to increase the antiferromagnetic contribution. It seems that when the carboxylate *anti-syn* bridges are short and equivalent, a overall ferromagnetic interaction is encountered, and the longer bridges are related to AF interactions. A point that need theoretical assessment.

Acknowledgements

Financial support from the Spanish Ministerio de Economía y Competitividad (MINECO) through projects MAT2010-16981, CTQ2010-15364, MAT2011-25991 and the Consolider-Ingenio projects, 'La Factoría' CSD2006-00015 and CSD2007-00010 and the Generalitat Valenciana project ISIC2012/002 are gratefully acknowledged. Pre-doctoral fellowships from MINECO (P. D-G.) and Agencia Canaria de Investigación, Innovación y Sociedad de la Información (C. M-B.) are acknowledged.

Notes and references

^a Laboratorio de Rayos X y Materiales Moleculares (MATMOL), Departamento de Física, Facultad de Ciencias, Universidad de La Laguna, Av. Astrofísico Francisco Sánchez s/n, 38206 La Laguna (Tenerife), Spain. jpasang@ull.edu.es, caruiz@ull.edu.es

^b Departament de Química Inorgànica, Universitat de La Laguna, Av. Astrofísico Francisco Sánchez s/n, 38204 La Laguna (Tenerife), Spain.

^c Institut Laue-Langevin, 71 avenue des Martyrs, C.S. 20156, 38042 Grenoble Cedex 9, France.

^d Centro Universitario de la Defensa de Zaragoza, Ctra. Huesca s/n, 50090, Zaragoza, Spain.

^e Instituto de Ciencia Molecular (ICMol) / Departament de Química Inorgànica, Facultat de Química, Universitat de València, Av. Dr. Moliner 50, 46100 Burjassot (València), Spain.

† From a CSD Search (CSD v. 5.35 Feb 2014) without restrictions; the basal plane defined by the donor atoms (O or N) with a constraint in the distance.

Electronic Supplementary Information (ESI) available: Crystallographic data in CIF format for **2-4** and **6-8** (CCDC 996269-996274). See DOI: 10.1039/b000000x/

- (a) H. Furukawa, K. E. Cordova, M. O'Keeffe, O. M. Yaghi, *Science*, 2013, **341**, 974; (b) E. Coronado and G. Mínguez-Espallargas, *Chem. Soc. Rev.* 2013, **42**, 1525; (c) J.-R. Li, J. Sculley and H.-C. Zhou, *Chem. Rev.* 2012, **112**, 869; (d) W.-M. Xuan, C.-F. Zhu, Y. Liu and Y. Cui, *Chem. Soc. Rev.* 2012, **41**, 1677.
- (a) C. P. Landee and M. M. Turnbull, *Eur. J. Inorg. Chem.* 2013, 2266; (b) M. Kurmoo, *Chem. Soc. Rev.* 2009, **38**, 1353; (c) E. Pardo, R. Ruiz-García, J. Cano, X. Ottenwaelder, R. Lescouëzec, Y. Journaux, F. Lloret and M. Julve, *Dalton Trans.* 2008, 2780.
- (a) G. Beobide, O. Castillo, J. Cepeda, A. Luque, S. Pérez-Yanez, P. Román and J. Thomas-Gipson, *Coord. Chem. Rev.* 2013, **257**, 2716; (b) F. A. Mautner, J. H. Albering, R. Vicente, C. Andrepont, J. G. Gautreaux, A. A. Gallo and S. S. Massoud, *Polyhedron*, 2013, **54**, 158; (c) C. N. R. Rao, S. Natarajan and R. Vaidhyanathan, *Angew. Chem. Int. Ed.* 2004, **43**, 1466; (d) M. Eddaoudi, D. B. Moler, H.-L. Li, B.-L. Chen, T. M. Reineke, M. O'Keeffe, O. M. Yaghi, *Acc. Chem. Res.* 2001, **34**, 319; (e) A. Rodríguez-Forteza, P. Alemany, S. Álvarez and E. Ruiz, *Chem. Eur. J.* 2001, **7**, 627.
- D. Ghoshal, T. K. Maji, G. Mostafa, S. Sain, T. H. Lu, J. Ribas, E. Zangrando and N. R. Chaudhuri, *Dalton Trans.* 2004, **11**, 1687.
- (a) C. Ruiz-Pérez, Y. Rodríguez-Martín, M. Hernández-Molina, F. S. Delgado, J. Pasán, J. Sanchiz, F. Lloret and M. Julve, *Polyhedron*, 2003, **22**, 2111; (b) H. El Bakkali, A. Castiñeiras, I. García-Santos, J. M. González-Pérez and J. Niclós-Gutiérrez, *Cryst. Growth Des.* 2014, **14**, 249; (c) Y. Rodríguez-Martín, M. Hernández-Molina, F. S. Delgado, J. Pasán, C. Ruiz-Pérez, J. Sanchiz, F. Lloret and M. Julve, *CrystEngComm* 2002, 522.
- (a) J. Pasán, F. S. Delgado, Y. Rodríguez-Martín, M. Hernández-Molina, C. Ruiz-Pérez, J. Sanchiz, F. Lloret and M. Julve, *Polyhedron*, 2003, **22**, 2143; (b) C. Ruiz-Pérez, J. Sanchiz, M. Hernández-Molina, F. Lloret and M. Julve, *Inorg. Chem.* 2000, **39**, 1363; (c) T. K. Maki, S. Sain, G. Mostafa, T. H. Lu, J. Ribas, M. Monfort and N. R. Chaudhuri, *Inorg. Chem.* 2003, **42**, 709; (d) F. S. Delgado, C. A. Jiménez, P. Lorenzo-Luis, J. Pasán, O. Fabelo, L. Cañadillas-Delgado, F. Lloret, M. Julve and C. Ruiz-Pérez, *Cryst. Growth Des.* 2012, **12**, 599; (e) F. S. Delgado, M. Hernández-Molina, J. Sanchiz, C. Ruiz-Pérez, Y. Rodríguez-Martín, T. López, F. Lloret and M. Julve, *CrystEngComm* 2004, **6**, 106.
- Methylmalonate: (a) J. Pasán, J. Sanchiz, F. Lloret, M. Julve and C. Ruiz-Pérez, *CrystEngComm* 2007, **9**, 478; (b) C. Gkioni, A. K. Boudalis, Y. Sanakis, C.P. Raptopoulou, *Polyhedron* 2007, **26**, 2536; (c) J. Pasán, J. Sanchiz, L. Cañadillas-Delgado, O. Fabelo, M. Déniz, F. Lloret, M. Julve and C. Ruiz-Pérez, *Polyhedron* 2009, **28**, 1802; (d) S. Pérez-Yañez, O. Castillo, J. Cepeda, J. P. García-Terán, A. Luque, P. Román, *Eur. J. Inorg. Chem.* 2009, 3889; (e) M. Déniz, J. Pasán, O. Fabelo, L. Cañadillas-Delgado, F. Lloret, M. Julve and C. Ruiz-Pérez, *New J. Chem.* 2010, **34**, 2515; (f) M. Déniz, J. Pasán, O. Fabelo, L. Cañadillas-Delgado, P. Lorenzo-Luis, F. Lahoz, D. López, C. Yuste, M. Julve and C. Ruiz-Pérez, *C. R. Chimie* 2012, **15**, 911; (g) M. Déniz, I. Hernández-Rodríguez, J. Pasán, O. Fabelo, L. Cañadillas-Delgado, C. Yuste, M. Julve, F. Lloret and C. Ruiz-Pérez, *Cryst. Growth Des.* 2012, **12**, 4505; (h) M. Déniz, I. Hernández-Rodríguez, J. Pasán, O. Fabelo, L. Cañadillas-Delgado, J. Vallejo, M. Julve, F. Lloret and C. Ruiz-Pérez, *CrystEngComm* 2014, **16**, 2766; (i) G. A. Farnum, J. A. Nettleman, R. L. LaDuca, *CrystEngComm* 2010, **12**, 888.
- (a) M. Déniz, J. Pasán, J. Ferrando-Soria, O. Fabelo, L. Cañadillas-Delgado, C. Yuste, M. Julve, J. Cano and C. Ruiz-Pérez, *Inorg. Chem.* 2011, **50**, 10765; (b) R. Baldomá, M. Monfort, J. Ribas, X. Solans and M. A. Maestro, *Inorg. Chem.* 2006, **45**, 8144.
- Phenylmalonate: (a) K.-L. Zhang, H.-W. Kuai and G.-W. Diao, *J. Mol. Struct.* 2006, **788**, 134; (b) J. Pasán, J. Sanchiz, F. Lloret, M. Julve and C. Ruiz-Pérez, *Polyhedron* 2011, **30**, 2451; (c) G.-H. Cui, J.-R. Li, T.-L. Hu and X.-H. Bu, *J. Mol. Struct.* 2005, **738**, 183; (d) J. Pasán, J. Sanchiz, C. Ruiz-Pérez, F. Lloret and M. Julve, *Inorg. Chem.* 2005, **44**, 7794; (e) J. Pasán, J. Sanchiz, C. Ruiz-Pérez, F. Lloret and M. Julve, *New J. Chem.* 2003, **27**, 1557; (f) J. Pasán, J. Sanchiz, C. Ruiz-Pérez, F. Lloret and M. Julve, *Eur. J. Inorg. Chem.* 2004, 4081.
- (a) W. B. Yang, A. Greenway, X. A. Lin, R. Matsuda, A. J. Blake, C. Wilson, W. Lewis, P. Hubberstey, S. Kitagawa, N. R. Champness and M. Schroder, *J. Am. Chem. Soc.* 2010, **132**, 14457; (b) S. O. H. Gutschke, D. J. Price, A. K. Powell and P. T. Wood, *Angew. Chem. Int. Ed.* 2001, **40**, 1920; (c) R. Kuhlman, G. L. Schimek and J. W. Kolis, *Inorg. Chem.* 1999, **38**, 194; (d) M. C. Etter, *J. Phys. Chem.* 1991, **95**, 4601; (e) S. K. Burley and G. A. Petsko, *Science* 1985, **229**, 23; (f) J. Singh and J. M. Thornton, *FEBS Lett.* 1985, **191**, 2989; (g) C. A. Hunter, J. Singh and J. M. Thornton, *J. Mol. Biol.* 1990, **211**, 595; (h) L. F. Lindoy and I. M. Atkinson, *Self-Assembly in Supramolecular Chemistry*, Royal Society of Chemistry, Cambridge, UK (2000); (i) I. Dance, *Supramolecular Inorganic Chemistry, in The Crystal as a Supramolecular Entity*, ed. G. R. Desiraju, John Wiley & Sons, Chichester, UK (1996).
- J. Pasán, J. Sanchiz, C. Ruiz-Pérez, J. Campo, F. Lloret and M. Julve, *Chem. Commun.* 2006, 2857.
- A. Earnshaw, *Introduction to Magnetochemistry*; Academic Press: London, 1968.
- A. J. M. Duisenberg, L. M. J. Kroon-Batenburg and A. M. M. Schreurs, *J. Appl. Crystallogr.* 2003, **36**, 220.
- Agilent CrysAlis Pro, Agilent Technologies Ltd., Yarnton, England, 2010.

- 15 G. M. Sheldrick, *Acta Cryst.* 2008, **A64**, 112.
- 16 L. J. Farrugia, *J. Appl. Crystallogr.* 1999, **32**, 837.
- 17 M. Nardelli, *J. Appl. Crystallogr.* 1995, **28**, 659.
- 18 DIAMOND 2.1d, Crystal Impact GbR, CRYSTAL IMPACT, K. Brandenburg and H. Putz GbR, Postfach 1251, D-53002 Bonn, Germany, 2000.
- 19 C. Janiak, *Dalton Trans.* 2000, 3885.
- 20 (a) P. A. Wood, S. J. Borwick, D. J. Watkin, W. D. S. Motherwell and F. H. Allen, *Acta Cryst.* 2008, **B64**, 393; (b) M. Kubicki, *Acta Cryst.* 2004, **B58**, o255.
- 21 F. H. Allen, C. A. Baalham, J. P. M. Lommerse and P. R. Raithby, *Acta Cryst.* 1998, **B54**, 320.
- 22 A. W. Addison, T. N. Rao, J. Reedijk, J. van Rijn and G. C. Verschoor, *Dalton Trans.* 1984, 1349.
- 23 F. S. Delgado, J. Sanchiz, C. Ruiz-Pérez, F. Lloret and M. Julve, *CrystEngComm* 2003, **5**, 280.
- 24 F. H. Allen, *Acta Cryst.* 2002, **B58**, 380.
- 25 F. F. Awwadi, R. D. Willett, K. A. Peterson and B. Twamley, *Chem. Eur. J.* 2006, **12**, 8952.
- 26 (a) F. F. Awwadi, R. D. Willett, S. F. Haddad, B. Twamley, *Cryst. Growth Des.* 2006, **6**, 1833; (b) G. Mínguez-Espallargas, L. Brammer, J. van de Streek, K. Shankland, A. J. Florence and H. Adams, *J. Am. Chem. Soc.* 2006, **128**, 9584; (c) G. Mínguez-Espallargas, J. van de Streek, P. Fernandes, A. J. Florence, M. Brunelli, K. Shankland and L. Brammer, *Angew. Chem. Int. Ed.* 2010, **49**, 8892.
- 27 G. S. Rushbrooke, G. A. Baker and P. J. Wood, *Phase Transitions and Critical Phenomena*, vol. III; C. Domb and M. S. Green, Eds., Academic Press, 1974.
- 28 W. E. Estes, D. P. Gavel, W. E. Hatfield and D. Hodgson, *Inorg. Chem.* 1978, **17**, 1415.
- 29 R. Navarro, *Application of High- and Low-Temperature Series Expansions to Two-dimensional Magnetic Systems*, L. J. de Jongh, Ed. Kluwer Academic Publishers, Dordrecht, 1990.
- 30 (a) Y.-Q. Zheng, X.-S. Zhai, L. Jin, H.-L. Zhu, J.-L. Lin and W. Xu, *Polyhedron* 2014, **68**, 324; (b) Y.-H. Liu, S.-H. Lee, J.-C. Chiang, P.-C. Chen, P.-H. Chien and C. Yang, *Dalton Trans.* 2013, **42**, 16857; (c) H. Arora, F. Lloret and R. Mukherjee, *Inorg. Chem.* 2009, **48**, 1158; (d) H. Arora, F. Lloret and R. Mukherjee, *Dalton Trans.* 2009, **44**, 9759; (e) J. Suárez-Varela, J. A. Mota, H. Aouryaghal, J. Cano, A. Rodríguez-Diéguez, D. Luneau and E. Colacio, *Inorg. Chem.* 2008, **47**, 8143; (f) E. Colacio, M. Ghazi, R. Kivekäs, J. M. Moreno, *Inorg. Chem.* 2000, **39**, 2882.
- 31 (a) J. C. Bonner and M. E. Fisher, *Phys. Rev. A*, 1964, **135**, 640; (b) R. L. Orbach, *Phys. Rev.* 1958, **112**, 309.
- 32 O. Kahn, *Molecular Magnetism*, VCH, New York, 1993.

Table 1. Crystallographic data for complexes 2-8

	2	3	4	6	7	8
Formula	C ₁₃ H ₁₀ O ₄ N ₂ Cu	C ₁₅ H ₁₀ O ₄ N ₂ Cu	C ₁₅ H ₁₀ O ₄ N ₂ Cu	C ₁₄ H ₁₀ O ₄ NClCu	C ₁₄ H ₁₀ O ₄ NBrCu	C ₁₄ H ₁₀ O ₄ NICu
FW	321.77	345.79	345.79	355.22	399.68	446.67
Crystal system	Monoclinic	Monoclinic	Monoclinic	Monoclinic	Monoclinic	Monoclinic
Space group	<i>P</i> 2 ₁ / <i>n</i>	<i>P</i> 2 ₁ / <i>n</i>	<i>P</i> 2 ₁ / <i>n</i>	<i>P</i> 2 ₁ / <i>n</i>	<i>P</i> 2 ₁ / <i>n</i>	<i>P</i> 2 ₁ / <i>n</i>
<i>a</i> / Å	7.019(3)	6.9188(8)	6.3297(2)	6.2264(11)	6.2413(2)	6.2716(2)
<i>b</i> / Å	28.604(3)	31.180(12)	31.7864(11)	30.6016(17)	31.0345(7)	31.9680(7)
<i>c</i> / Å	5.964(3)	6.2103(11)	6.9390(2)	6.9804(12)	6.9777(2)	6.9916(2)
β / °	91.808(8)	93.463(15)	92.732(3)	93.297(13)	93.573(2)	93.949(2)
<i>V</i> / Å ³	1196.8(8)	1337.3(6)	1394.53(8)	1327.8(3)	1348.92(7)	1398.42(7)
<i>Z</i>	4	4	4	4	4	4
μ / mm ⁻¹	1.840	1.653	2.406	1.860	5.908	19.686
<i>T</i> / K	293(2)	293(2)	293(2)	293(2)	293(2)	293(2)
ρ_{calc} / g cm ⁻³	1.786	1.717	1.647	1.777	1.975	2.122
λ / Å	0.71073	0.71073	1.54184	0.71073	1.54184	1.54184
Index ranges	-9 ≤ <i>h</i> ≤ 9, -36 ≤ <i>k</i> ≤ 36, -7 ≤ <i>l</i> ≤ 7	-9 ≤ <i>h</i> ≤ 9, -43 ≤ <i>k</i> ≤ 43, -8 ≤ <i>l</i> ≤ 8	-7 ≤ <i>h</i> ≤ 6, -35 ≤ <i>k</i> ≤ 38, -6 ≤ <i>l</i> ≤ 8	-7 ≤ <i>h</i> ≤ 8, -42 ≤ <i>k</i> ≤ 38, -9 ≤ <i>l</i> ≤ 9	-7 ≤ <i>h</i> ≤ 6, -38 ≤ <i>k</i> ≤ 37, -8 ≤ <i>l</i> ≤ 6	-6 ≤ <i>h</i> ≤ 7, -39 ≤ <i>k</i> ≤ 39, -8 ≤ <i>l</i> ≤ 8
Indep. reflect. (<i>R</i> _{int})	2694 (0.0753)	3787 (0.0986)	2727 (0.0219)	3721 (0.0659)	2648 (0.0357)	2780 (0.0500)
Obs. reflect. [<i>I</i> > 2σ(<i>I</i>)]	2240	2718	2393	2168	2448	2588
Parameters	181	199	199	190	190	190
Goodness-of-fit	1.214	1.013	1.028	1.148	1.184	1.181
<i>R</i> [<i>I</i> > 2σ(<i>I</i>)]	0.0600	0.0578	0.0323	0.0876	0.0574	0.0491
<i>R</i> _w [<i>I</i> > 2σ(<i>I</i>)]	0.1327	0.1369	0.0827	0.1791	0.1675	0.1364
<i>R</i> (all data)	0.0742	0.0865	0.0380	0.1535	0.0604	0.0524
<i>R</i> _w (all data)	0.1280	0.1475	0.0867	0.1960	0.1707	0.1392

Table 2. Magneto-structural details for layered R-malonate complexes.

Compound	$d_1^a / \text{\AA}$	$\gamma^b / ^\circ$	$\beta^c / ^\circ$	$d_2^d / \text{\AA}$	J / cm^{-1}	g	Model ^e	Ref.
1	5.100(8) 5.143(7)	60.57(2)-72.62(2) 59.76(3)-71.28(2)	63.16(2)	13.45(4)	+ 5.6(1) ^c	2.12(2)	2D-Heisenberg-F	11
2	5.058(3) 5.187(3)	53.915(8)-68.299(8) 53.749(8)-67.081(9)	66.761(12)	12.413(3)	+10.4(1) / -3.19(5)	2.072(4)	1D-F + mean field	This work
3	4.984(2) 5.238(2)	49.694(7)-72.921(7) 48.941(7)-67.752(7)	71.168(6)	13.705(3)	+6.3(1) / -0.82(1)	2.052(2)	1D-F + mean field	This work
4^f	5.022(5) 5.229(4)	46.77(2)-70.56(2) 47.69(2)-73.08(2)	71.725(14)	14.039(1)	+1.69(2) / -0.26(1) +6.0(1) / +0.070(4)	2.14(2) 2.060(5)	2D-Heisenberg-F 1D-F + mean field	This work
6^f	5.0152(13) 5.2585(14)	49.1(4)-72.6(3) 48.5(4)-68.3(3)	71.36(11)	13.534(7)	-0.91(3) / +0.27(3)	2.059(1)	1D-AF + mean field	This work
7	5.0059(8) 5.2691(8)	48.2(1)-73.2(2) 47.9(2)-68.4(2)	71.55(5)	13.7673(9)	+6.3(1) / -0.929(2)	2.076(2)	1D-F + mean field	This work
8	5.0028(9) 5.296(1)	48.5(3)-73.5(2) 47.6(3)-68.7(3)	71.21(8)	14.278(2)	+6.8(1) / -1.089(3)	2.055(2)	1D-F + mean field	This work
[Cu(Memal)(H₂O)]_n	4.9653(12)	29.3(3)-82.4(2)	84.44(9)	6.203(3)	+1.61(1)	2.20(3)	2D-Heisenberg-F	7a
[Cu(μ-cbdca)(H₂O)]_n	4.842(5)	33.3(2)-61.88(18)	82.3(5)	8.481(3)	+4.76	2.14	2D-Heisenberg-F	8b

^a Intralayer copper-copper separation through each one of the crystallographically independent carboxylate-bridges.

^b Dihedral angle between the basal plane of the copper(II) ion and the plane of the carboxylate bridge for each independent pathway [O(1)-C(1)-O(2) and O(3)-C(3)-O(4)]. The two values per bridge correspond to the *anti* and *syn* sides, respectively.

^c Dihedral angle between the mean basal plane of carboxylate-bridged copper(II) ions.

^d Shortest interlayer Cu...Cu separation.

^e Model used to fit the magnetic experimental data. 2D-Heisenberg-F (eq. 4; ref. 29); 1D-F + mean field (eqns. 1-3; refs. 27,28); 1D-AF + mean field (eq. 5; ref. 31).

^f Compound **4** is presented with two alternative models for the analysis of the magnetic data (see text).

FIGURES

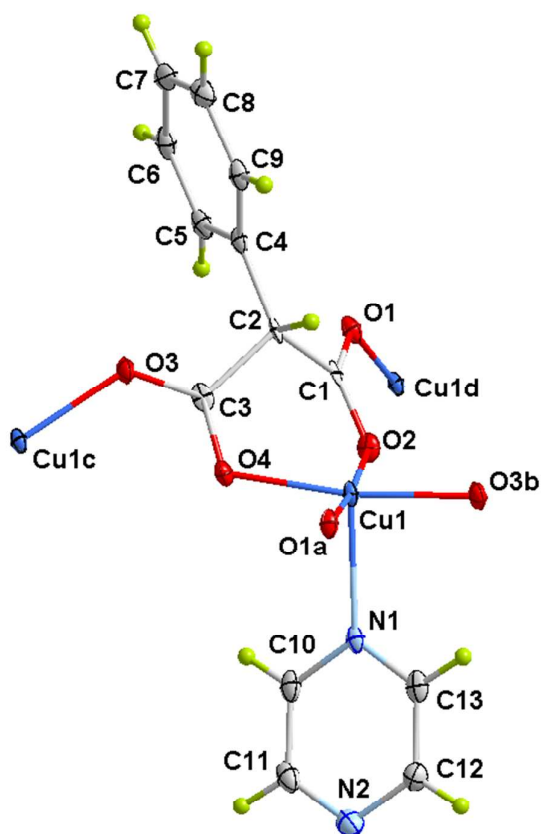


Figure 1. A view of a fragment of the crystal structure of **2** along with the atom numbering scheme. Ellipsoids are represented at 50% probability. Symmetry codes: (a) $x - 1/2, -y + 1/2, z - 1/2$; (b) $x + 1/2, -y + 1/2, z - 1/2$; (c) $x - 1/2, -y + 1/2, z + 1/2$; (d) $x + 1/2, -y + 1/2, z + 1/2$.

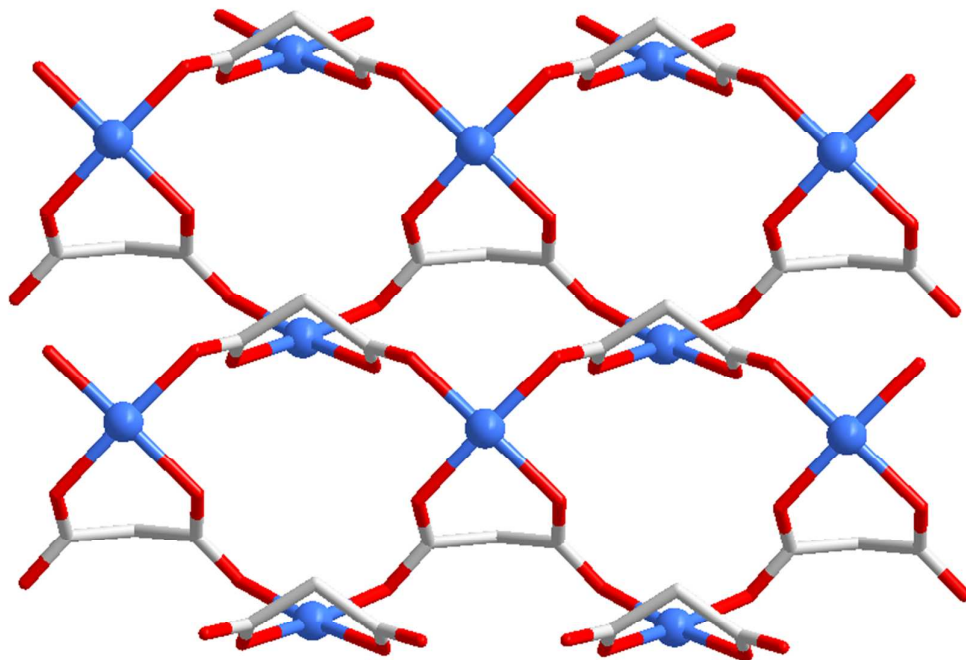


Figure 2. View of the corrugated square grid of copper(II) ions of the structures of **1-8**. The *anti-syn* carboxylate bridges are in out-of-plane conformation linking equatorial positions of the copper(II) environments.

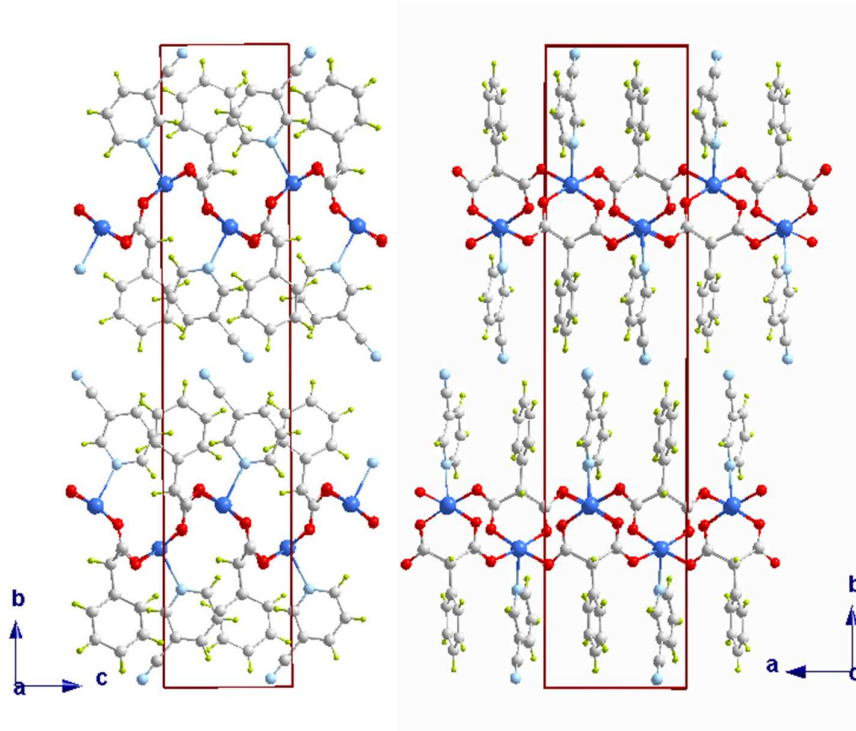


Figure 3. The crystal packing of compound **3** along the crystallographic *a* (left) and *c* directions (right). The unit cell edges are presented in dark red colour. The layers are twisted following an *ABABAB* sequence along the *b* axis.

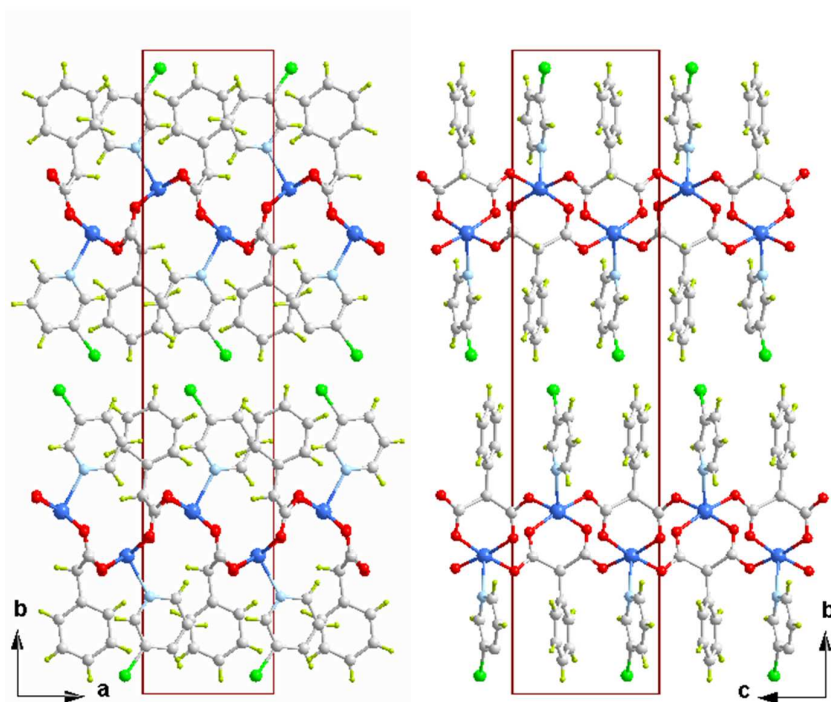


Figure 4. The crystal packing of compound **6** along the crystallographic *c* (left) and *a* directions (right). The unit cell edges are presented in dark red colour. The layers are twisted following an *ABABAB* sequence along the *b* axis.

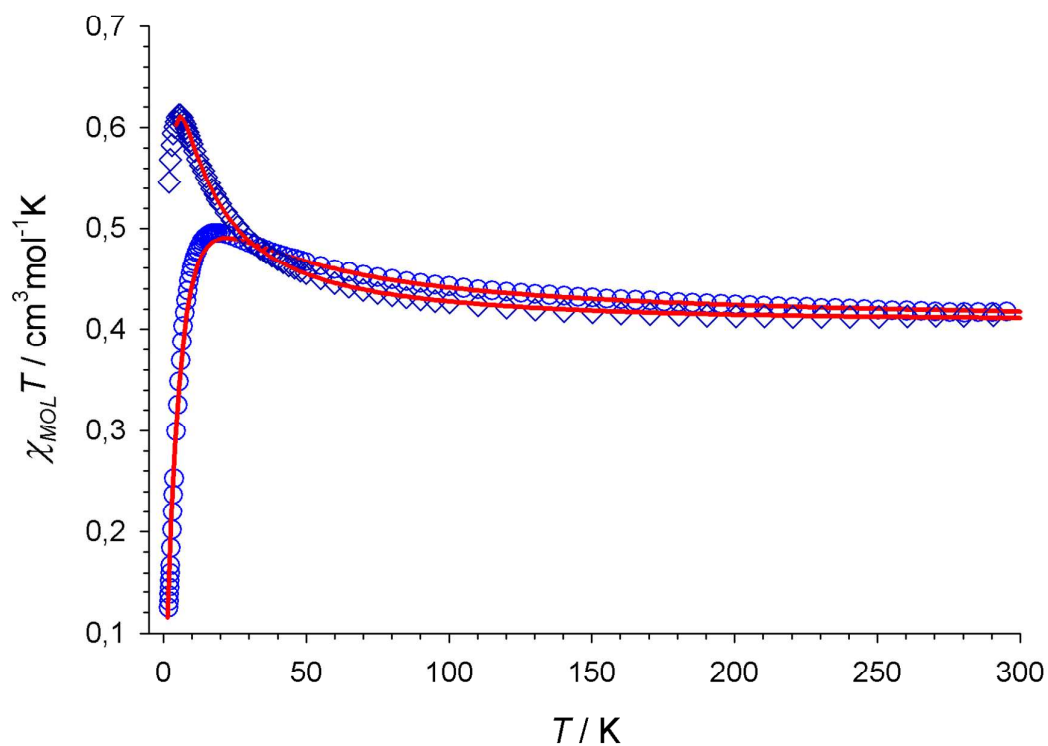


Figure 5. The temperature dependence of the $\chi_M T$ products for the complexes **2** (circles) and **3** (diamonds) in the temperature range 1.9-300 K. The lines represent the best fit (see text).

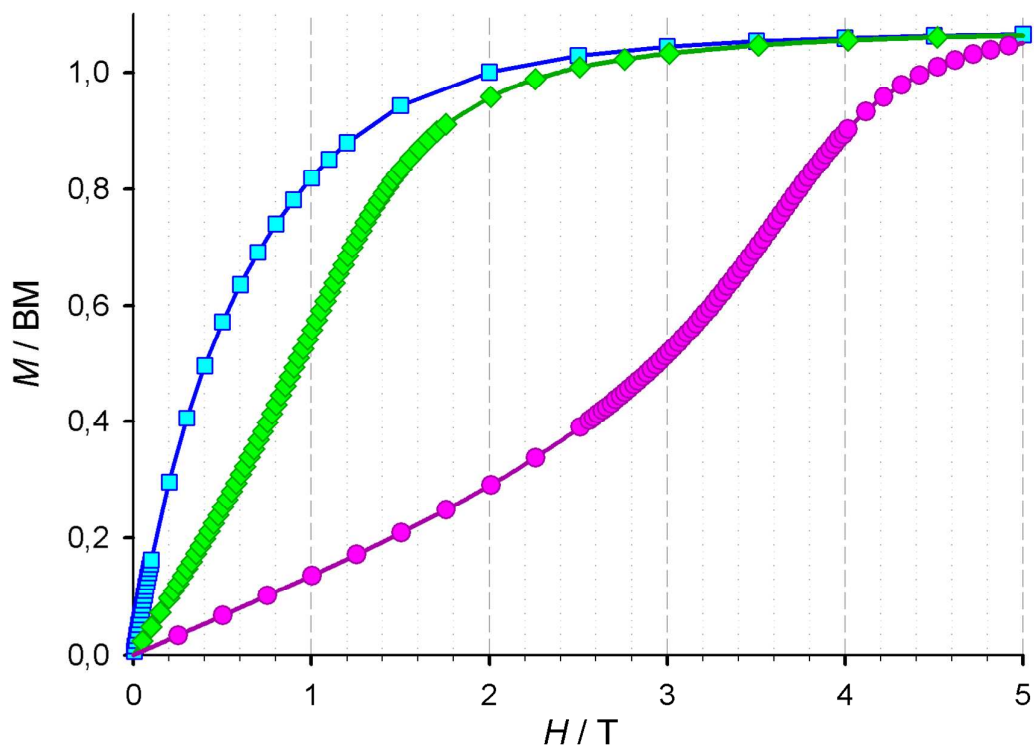


Figure 6. Magnetization vs. magnetic applied field plots at 2 K for **2** (pink circles), **3** (green diamonds) and **4** (blue squares). The lines are only an eye-guide.

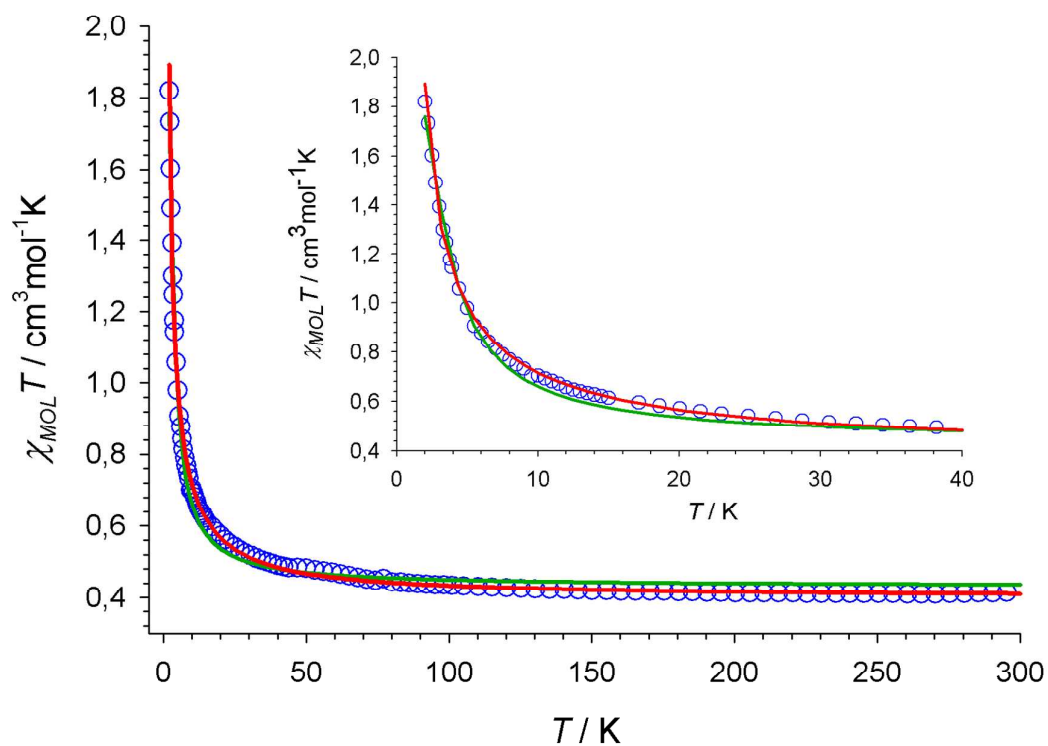


Figure 7. The temperature dependence of the $\chi_M T$ products for the complex **4** in the temperature range 1.9-300 K. The line represents the best fit through eqn. 4 (green) and eqns. 1-3 (red; see text). The inset shows the low temperature region in detail.

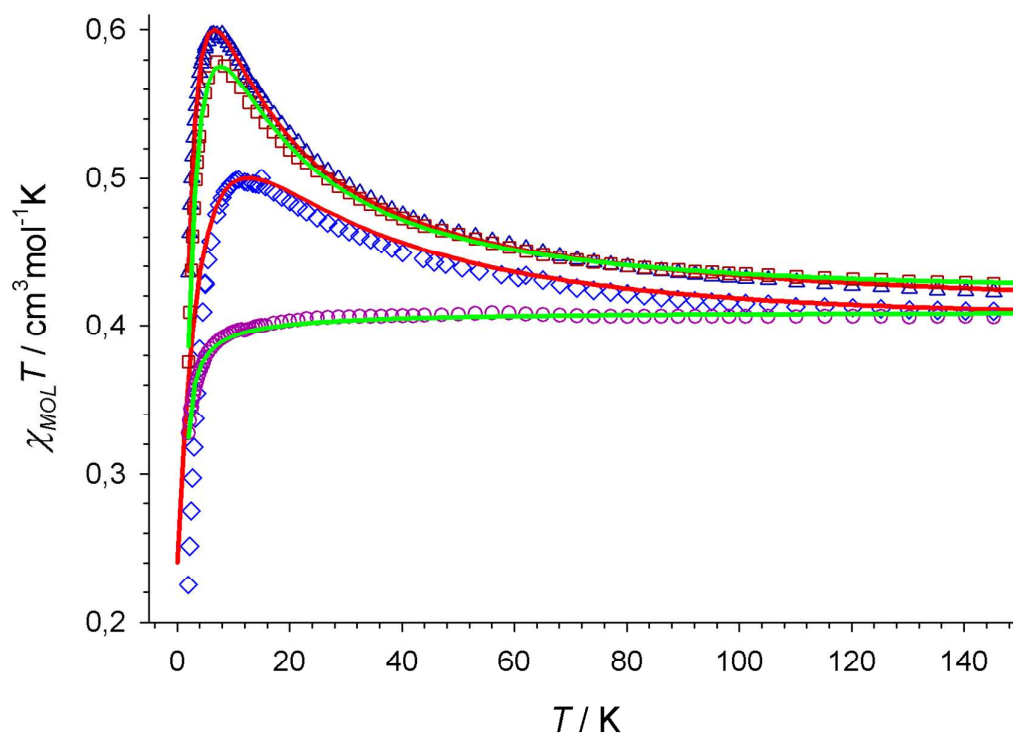


Figure 8. The temperature dependence of the $\chi_M T$ products for the complexes **5** (blue diamonds), **6** (purple circles), **7** (blue triangles) and **8** (red squares) in the temperature range 1.9-150 K. The lines represent the best fit (see text).

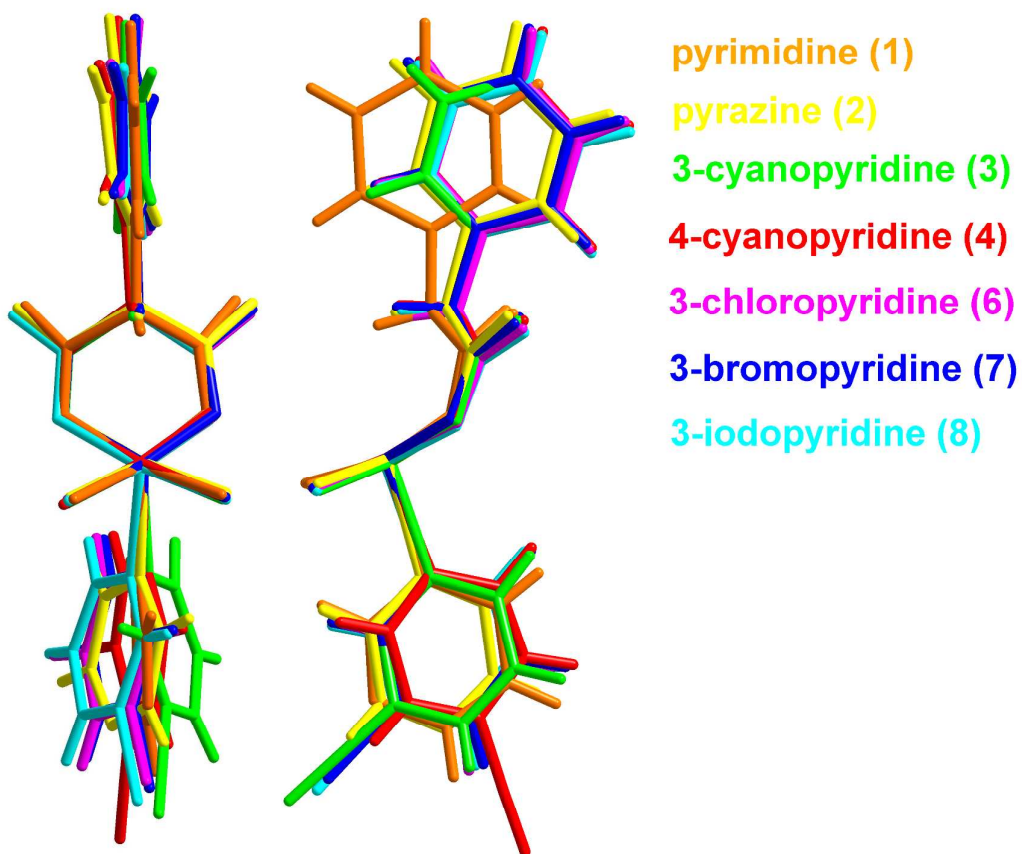


Figure 9. Two different views of a superposition of the same structural fragment for compounds **1-4** and **6-8**. The copper(II) atom is the anchoring position and the basal plane of the copper environment has been locked for comparison purposes.

Table of Contents

for the manuscript:

Influence of the coligand in the magnetic properties of a series of copper(II)-phenylmalonate complexes

Jorge Pasán,^{a,*} Joaquín Sanchiz,^b Óscar Fabelo,^c Laura Cañadillas-Delgado,^d Mariadel Déniz,^a Pau Díaz-Gallifa,^a Carla Martínez-Benito,^a Francesc Lloret,^e Miguel Julve^e and Catalina Ruiz-Pérez^{a,*}

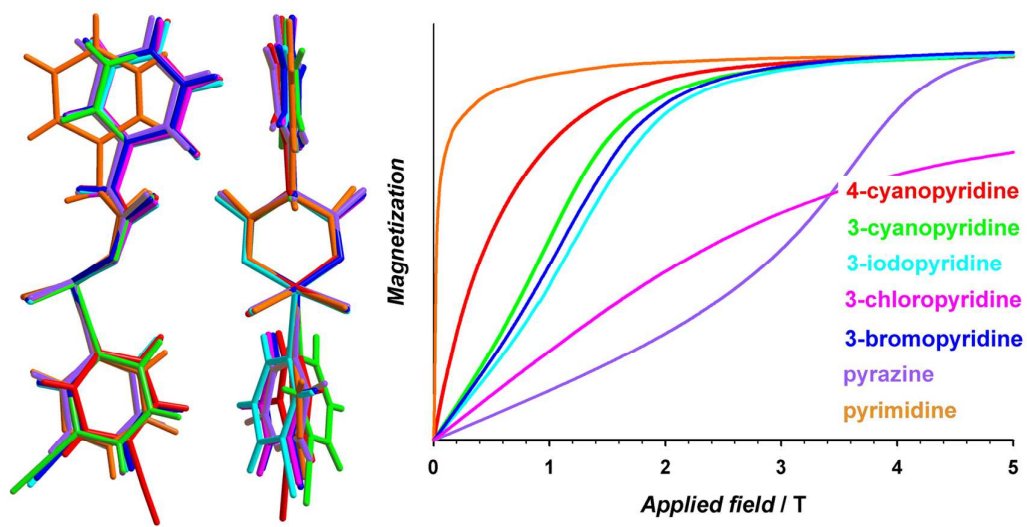
^aLaboratorio de Rayos X y Materiales Moleculares (MATMOL), Departamento de Física, Facultad de Ciencias, Universidad de La Laguna, Av. Astrofísico Francisco Sánchez s/n, 38206 La Laguna (Tenerife), Spain. jpasang@ull.edu.es, caruiz@ull.edu.es

^bDepartamento de Química Inorgánica, Universidad de La Laguna, Av. Astrofísico Francisco Sánchez s/n, 38204 La Laguna (Tenerife), Spain.

^cInstitut Laue-Langevin, Grenoble, 71 avenue des Martyrs, C.S.20156, 38042 Grenoble Cedex 9, France.

^dCentro Universitario de la Defensa de Zaragoza. Ctra de Huesca s/n. 50090, Zaragoza, Spain.

^eInstituto de Ciencia Molecular(ICMol) / Departament de Química Inorgànica, Facultat de Química, Universitat de València, Av. Dr. Moliner 50, 46100 Burjassot (València), Spain.



The magnetic properties of a series of copper(II)-phenylmalonate complexes are tuned by the pyridine-type coligand.